Journal of Multidisciplinary Engineering Science Studies (JMESS)
ISSN: 2458-925X
Vol. 7 Issue 9, September - 2021

Using Chitosan Nanosilica Composite For Removal Of Some Heavy Metals From Water Resources

Ahmed.M. Desouky[a], Mohamed E.A. Ali[a], Hesham A. Ezzeldin[a], Ahmed Shahat[b]
[a] Hydrogeochemistry department, Desert Research Center, Cairo, Egypt
[b]Department of Chemistry, Faculty of Science, Suez University, Suez, Egypt
E-mail address: ahmeddesouky_27@hotmail.com

Abstract*—This study examined the removal of heavy metal ions with taking in the consideration of ($Cu^{2+}$and Zn^{2+}) from aqueous solutions and/or groundwater by adsorption technique using chitosan-mesoporous silica composite. In the present study, we combined Mesoporous silica nanoparticles (MSN) and chitosan in order to take the advantage of high surface area and pore volume of MSN, namely exhibits highly efficient adsorption capacity. The derived material has been characterized by a variety of techniques such as Fourier transform infrared (FTIR), scanning electron microscope (SEM), and X-ray (X-RD). Based on the adsorption-regeneration recyclability, the results indicate that the prepared chitosan- mesoporous silica composite material possesses good stability and reusability for adsorption.

Keywords— Nanoparticles; Silica; Chitosan; Water treatment; Heavy metals Removal

I. INTRODUCTION

Water pollution caused by heavy metals is an environmental problem that raises concerns all over the world. Sorbent materials are of great importance for the removal of these metals. Nevertheless owing to reduced size, most sorbents are difficult to collect from water and therefore there is need to develop effective sorbents that could be easily separated from aquatic environments [1]. Nano-adsorbents possess two main properties: innate surface and external functionalization. Their physical, chemical and material properties are also related to their extrinsic surface structure, apparent size and intrinsic composition [2]. The high surface area and pore volume, the controllable of pore size and morphology, and also the ease of surface modification have attracted much attention of researchers around the world to study these materials for various applications. Among previous studies, the observation of nanoporous silica based materials as heavy metals carriers is one of the most active research area [3]. Recently, adsorption technique has emerged as an economic and efficient technique for dyes and heavymetals removal from contaminated aqueous solutions, particularly with low concentration solutions [4, 5]. Polysaccharides based hybrid materials have recently utilized as an economic and efficient adsorbents for waste water purification [6,7]. Furthermore, several investigations were focused on mesoporous silica functionalized with organic groups [8,9]. Many chemical molecules containing useful functional groups such as pyridine [10], poly(diallyl dimethylammonium chloride) [11]. In this study, a novel chitosan/silica nano composite was prepared, characterized and investigated for metal ions removal.

2.EXPERIMENTAL

2.1.Materials:

Chitosan (Aldrich, Germany), acetic acid (AAc) Mollin Ckrodt Company of purity 99% was used as received. The other chemicals, such as solvents, inorganic salts, organic compounds, and other reagents were used without further purification.

Synthesis of mesoporous silica nanospheres (MSN)

The synthesis of mesoporous silica products was achieved by the ammonia-catalyzed hydrolysis of TEOS (Tetraethyl orthosilicate)in a mixed solvent of water, diethyl ether and acetone using CTAB (cetyltrimethyl ammonium bromide) as a template at room temperature as described before. Typically, 0.5 g of CTAB was dissolved in 100 ml of water and stirred for 30 min, followed by adding 40 g of acetone and stirred for 30 min, then, we added 20 g diethyl ether. After vigorous stirring for 30 min, 2.5 g of TEOS was added and stirred for more 30 min, followed by adding 1.5 g NH_3 (25 *wt*.%). The resulting gel was vigorously stirred in a closed vessel at room temperature for 24 h. The particles were collected by filtration, cleaned with deionized water and dried at 80 °C for 24 h. Then they were calcined from room temperature to 550 °C for 4 h.; followed by heating at 550 °C for 8 h more.

2.2. Chitosan/silica composite preparation

First 0.1 g MSN was dispersed in 10 mL dimethyl formamide (DMF) for 15 min at room temperature. Then, 0.5 ml epichlorohydrin was added drop-wise to the solution at room temperature for 1 h. After the completion of reaction, the mixture was filtered and, to remove unreacted epichlorohydrin, was washed several times with 25% ethyl alcohol. Finally, modified MSN were kept wet for further reaction. The next step is the binding of chitosan on to the functionalized MSN surface via reaction of epoxy unit on MSN surfaces. MSN-epoxy was dispersed in acetic acid (0.1 g MSN epoxy, 10 mL for 2%), and chitosan (w/w) in acetic acid (2 g chitosan, 30 mL for 2%) was added to the MSN-epoxy solution and stirred for 24 h. MSN epoxy-Chitosan was precipitated due to cross-linking. The precipitate was washed with water/methanol solution several times, filtered, and dried at 40 °C.

2.3. Characterization of modified chitosans

The formation of additional nano particles groups on chitosan surface after modification with nano silica was studied using X-ray and FTIR-spectroscope type Nicolet Nexus 8700 (USA). Infrared spectra (FTIR) were obtained with a Perkin-Elmer spectrum. The chitosan and modified chitosan were dried overnight at 60 ◦C under reduced pressure and pressurized with a glass slide on top of the quartz window of the ATR instrument. High angle X-ray diffraction (XRD) patterns were recorded on X-ray diffractometer (D/Max2500VB2+/Pc, Rigaku, Japan) with Cu Kα characteristic radiation (wavelength = 0.154 nm) at a voltage of 40 kV and a current of 50 mA. The scanning scope of 2θ was from 0◦ to 70◦ at room temperature

2.4. Batch adsorption tests

Applicability of modified chitosans for Cu(II) and Zn(II) removal was studied using batch experiments in a reaction mixture of 0.1 g of adsorbent and 0.025 L of metal solution containing Cu(II) and/or Zn (II) at concentrations ranging from 200 to 1000 mgL^{-1}. The effect of pH was studied at metal concentration of 1000 mgL^{-1} in the pH range of 2–5. Alkaline solutions were not used to avoid the hydroxide formation (Orion 2 star pH Bench top "Thermo"). The effect of contact time was studied at metal concentrations of 200 mgL^{-1}. Agitation was undertaken using a rotary shaker type SK 300 (Lab companion). At designated contact time, the adsorbent was separated from the solution. The metal concentrations in the filtrates were analyzed by Atomic Absorption Spectrophotometer, (Unicam model Solar 929. The adsorption capacities (mg g^{-1}) of modified chitosan were calculated as follows:

$$qe = (C_i - C_e)\, V(L)/W$$

where C_i and C_e are the initial and the equilibrium concentrations, respectively (mg L^{-1}), while W(g) and V (L) represent the weight of the adsorbent and the volume of the solution, respectively.

2.5. Regeneration studies

To evaluate their reusability, regeneration of the spent adsorbents were performed in acidic conditions. At first, adsorbent were loaded by metal ions by mixing around 0.1 g of the adsorbent with 0.025 L of 1000 mgL^{-1} Cu(II) or Zn(II) solution. Regeneration studies were performed using higher metal ions concentrations to make separation procedure easier. After attaining equilibrium, the spent adsorbent was separated from the solution by centrifuge. Metal ions were eluted using 2M HNO_3. The regeneration efficiency (%RE) of the adsorbent was calculated using the following Eq:

$$\%RE = (q_r/q_0) \times 100$$

where q_0 and q_r are the adsorption capacities of the adsorbents (mg g^{-1}) before and after regeneration, respectively.

3. Results and discussion

3.1. Characterization of modified chitosans

FT-IR spectroscopy

The functional groups present in the chitosan and chitosan/silica hybrid materials were monitored by FT-IR spectroscopy as shown in Figure 1. Chitosan exhibits characteristic band at 3373 cm^{-1} which assigned to NH, OH symmetric stretching vibration (Figure 1A). In addition, characteristic signals at 1590 and 1460 cm^{-1} may attributed to C- O stretching (amide I) and -NH stretching (amide II), respectively [12]. Also, the occurrence of new vibrational bands suggests the formation of covalent linkages between MNS and chitosan. Thus, in the Si-Chitosan spectrum (Figure 1B) new bands appear at most intense bands

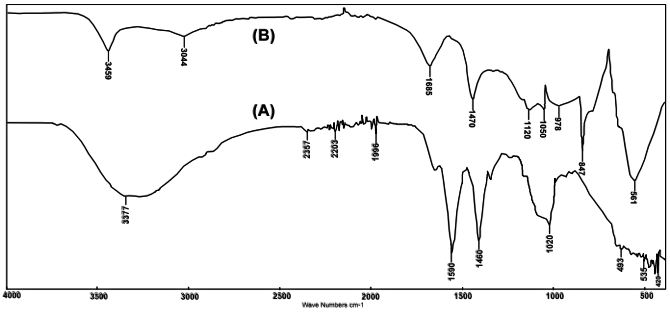

Figure 1 **Fig. 1 IR shows of the samples (A) chitosan and (B) chitosan - silica composite**

in the chitosan/silica hybrid was found between 1120 and 1050 cm^{-1} and can be associated with the Si-O-Si and Si-O-C vibrations. This band confirms that the hybridization went well. The peak at 978 cm^{-1}, assigned to Si-OH stretch, is shifted from 1020 cm^{-1} by hydrogen-bonding interactions. New peak at 561 cm^{-1} in the chitosan/silica nanocomposite was assigned to the stretching vibration of silica [13].

3.2.SEM and TEM analysis

The surface morphology of chitosan/silica nanocomposite was investigated using SEM analysis. Figure 2A shows that the surface morphology of the nanocomposite is relatively homogenous. The formed silica layer shows the existence of microplates with ~5 μm length. These plates consist of silica nanoparticles with diameter ~325 nm as shown in Figure 2B. Silica nanoparticles appear to be more distinct and uniform, due to the interaction between the chitosan/silica Hybrid nanoparticles that decreases the attractive forces between nanoparticles and reducing their aggregation tendency. Direct proof of the chitosan/silica nanocomposite configuration is given by transmission electron microscopy (TEM) as shown in Fig. 2B.The nano composite is homogeneous and consists of densely packed nanosphere with ~305.8 nm mean diameter.

3.3.X-ray diffraction studies

X-ray diffractometer was used to obtain the X-ray diffraction pattern with Cu K_ radiation being the source of X-ray at a setting of 30 kV and 30 mA. The 2Θ for the XRD pattern is recorded within the range of 0° - 70° at a scan rate of 2° per min. Fig 2 is a presentation of the XRD patterns of the chitosan and chitosan composites with MSN. Fig. 3a. Pure chitosan showed a strong peak at 19.5° as reported in the literature [14]. The intensity of this peak decreased Fig.

3b, which indicates that chitosan-functionalized with silica nanocomposites was more amorphous in nature.

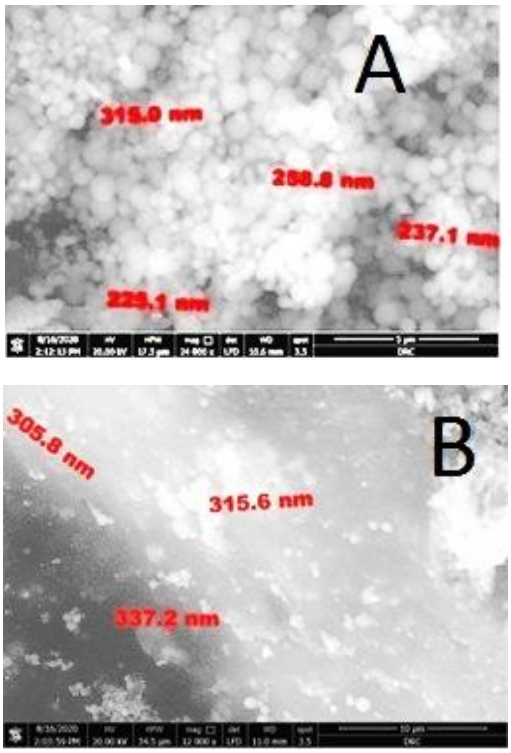

Figure 2 Scanning electron microscope images of Chitosan/silica and silica nanoparticles.

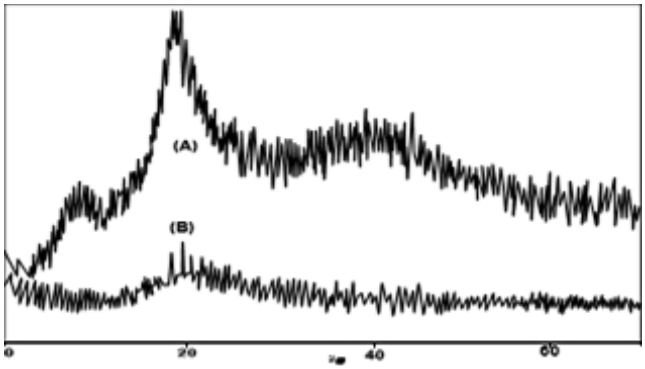

Figure 3 X-Ray diffraction patterns (XRD) of (A) Chitosan, (B) Chitosan/silica composite.

3.4. Effect of contact time

The capacity of Chitosan/silica composite was determined by varying the contact time in the range of 10–110 mins. About 0.1 g of the sorbent was placed into 50 ml of the 10 mg/L initial Cu(II) or Zn(II) solutions. The flasks with their contents taken for the study were shaken thoroughly using a mechanical shaker at 200 rpm. All the flasks were removed from the shaker and the contents were filtered and analyzed for Cu (II) and Zn (II), Figure 4.

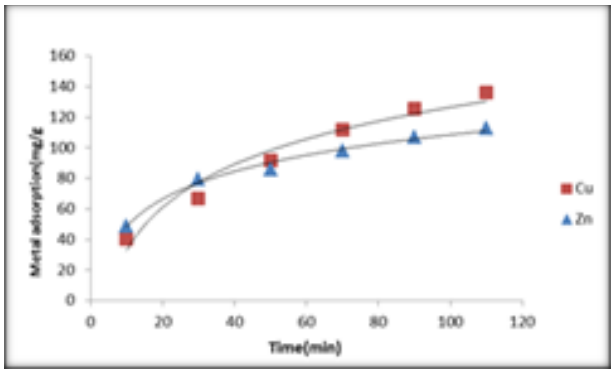

Figure 4 Metal uptake removal percent of the dissolved ions as a function of time

3.5. Effect of pH

The removal of ion from aqueous solution was highly dependent on the solution pH in many cases as it altered the surface charge on the sorbent. Therefore, Chitosan/silica composite sorbent was determined at fur different pH levels such as 2, 3, 4, and 5. The results are shown in Figure 5. It is obvious from the figure that the pH has a slight influence on the Chitosan/silica composite sorbents. A maximum metal uptake was observed at pH 5 and a slight decline in metal uptake was observed in acidic pH, the predominant species under acidic conditions, the surfaces of all the sorbents were highly protonated which unsuitable for uptake of Cu (II) or Zn (II), with the increase in pH, the degree of protonation of surface reduces gradually [15].

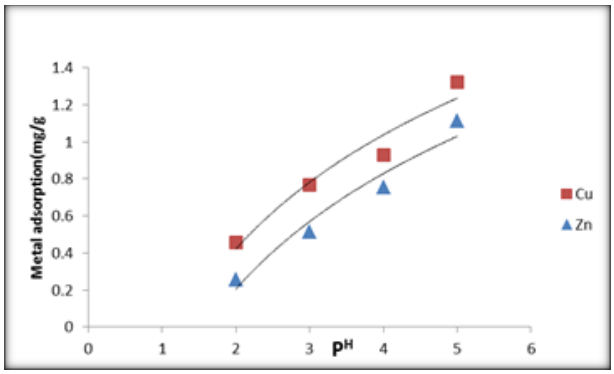

Figure 5 Metal uptake of the metal ions as a function of pH-dependent

3.6. Modeling of adsorption kinetics

Modeling of adsorption kinetics was conducted by using the pseudo-first-order and pseudo-second-order models. These originally empirical models have been used extensively to describe the sorption kinetics. Recently, also theoretical backgrounds for these models have been studied [16] using the classical Theory of Activated Adsorption/Desorption using the Statistical Rate Theory [17, 18]. The pseudo-first-order, (figure 6) model is expressed as [19]:

$$log(qe - qt) = log(qe) - k_1/2.303t$$

The coefficients of the pseudo-first-order and pseudo-second-order models obtained were presents in Table 1. The R^2 values of the pseudo-first-order

model exceeded 0.94 while for the second-order were about 0.98.

Table. 1. Pseudo-First order and pseudo-second order parameters for the adsorption of Cu (II) and Zn (II) on chitosan- silica composite.

Metal	$q_{e,cal}$ (mg/	$q_{e,exp.}$ (mg/	$K_1 \times 10^{-2}$	R^2	$q_{e,cal.}$ (mg/	$q_{e,exp.}$ (mg/	$K_2 \times 10^{-2}$ (gmg^{-1}	R^2
Cu^{2+}	51.3	102	0.39	0.94	103	102	0.176	0.985
Zn^{2+}	35.6	88	0.18	0.95	83	88	0.196	0.983

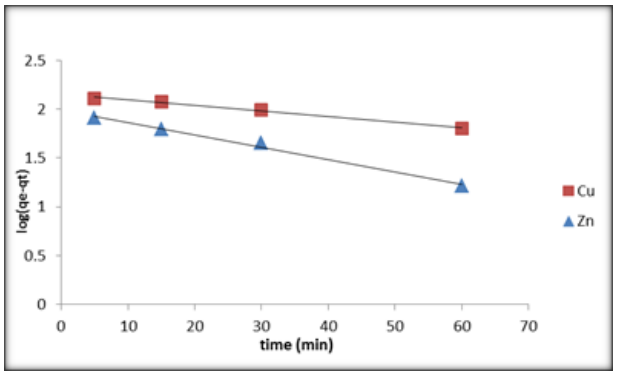

Figure 6 Plots of log(qe-qt) ainst time for the exchange of Cu (II) and Zn(II) ions on Chitosan- silica composite.

The pseudo-second-order rate equation is [19]:

$$t/q_t = 1/k_2 q_e$$

where qt and q_e (mg/g) are the adsorption capacity at time t and at equilibrium, respectively, while k_1 (min^{-1}) and k_2 (gmg^{-1} min^{-1}) are the pseudo-first-order and pseudo-second-order rate constants. Table 1 indicate that pseudo-first-order model was not representative to describe the experimental data.

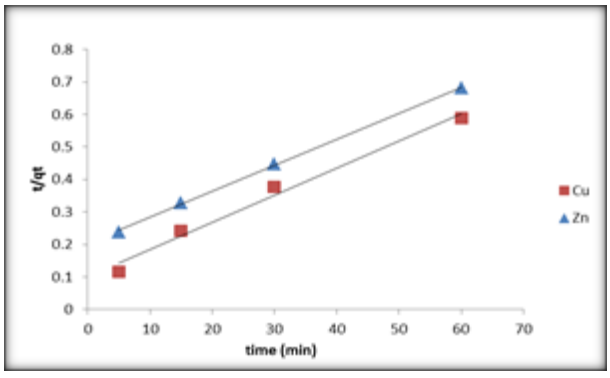

Figure 7 Pseudo second order model for the exchange of Cu (II) and Zn(II) ions on Chitsan- silica composite.

This could be due to the fact that pseudo-first-order model is generally applicable only at initial stage of adsorption [19,20]. However, according to Table 1, it is evident that the pseudo-second-order model gave the best fit to the experimental data since qe, exp and qe, model were very close to each other, (Figure 7). Thus, the main process resistance could be related to the kinetics of the sorption process [19]. Furthermore, the sorption fits better to the pseudo-second-order model than to the first-order model when the initial concentration of the adsorbate is not excessively high, which was also the case in this study [16].

3.7.Modeling adsorption isotherms.

Adsorption isotherms represent the adsorption capacity of the adsorbent as a function of adsorbate concentration in the solution at equilibrium conditions. To quantify the sorption capacity of the sorbents studied for heavy metal removal, the two most commonly used isotherms, namely Freundlich and Langmuir isotherms have been adopted. Langmuir, Freundlich, were chosen for equilibrium calculations since they are commonly used in description of liquid–solid systems [21]. The Langmuir model assumes a monolayer adsorption on a homogenous surface where the binding sites have the same adsorption affinity and no interactions between adsorbates are considered [21]:

$$\frac{Ce}{qe} = \frac{1}{Qob} + \frac{1}{Qo}\,Ce$$

where q_e (mg g^{-1}) and C_e (mg L^{-1}) are the adsorption capacity and the equilibrium concentration of the adsorbate, respectively, Q_o (mg g^{-1}) is the maximum adsorption capacity of adsorbents , Langmuir isotherm constants Q_o and b for Chitosan/silica composite were determined from the respective slope and intercept of the linear plot of Ce/qe vs. Ce (Figure 8).

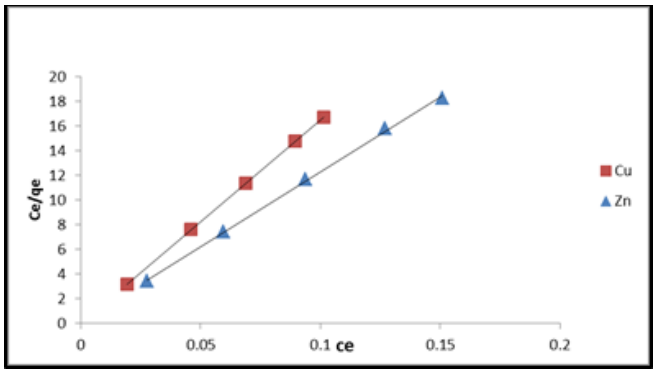

Figure 8 plot of (C_e/q_e) against Ce for Cu (II) and Zn(II) metals ions.

These values are presented in Table 2. The higher values of r indicate its applicability of Langmuir isotherm. The values of Q_o for all the sorbents increased with the increase in temperature. This confirms the endothermic nature and temperature dependence of the sorption process., while R_L (Lmg^{-1}) represents the energy of the adsorption. It can be given by :

$$R_L = \frac{1}{1+bCo}$$

Where b (L/mg) is Langmuir constant. It is found that the parameter R_L ($0 < R_L < 1$) shows favorable adsorption. Correlation coefficient (R^2) of Cu(II) and Zn(II) has been found to be 0.99 and 0.98,respectively (Table 2), indicating, also that adsorption of Cu(II) and Zn(II) is favorable at operation conditions studies.

Freundlich isotherm constants for Chitosan/silica composite was calculated from the linear plot of log qe

vs. log Ce (Figure 9) and the values are presented in Table 2. It shows that the Freundlich model correlated quite well with the experimental data for both Cu(II) and Zn (II) adsorption.

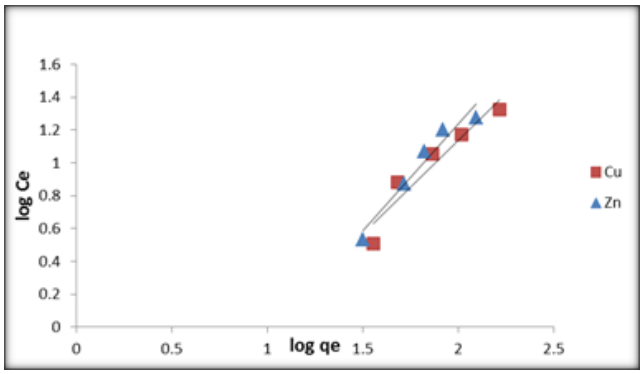

Figure 9 plot of log q_e versus log C_e for Zn (II) and Pb(II) metals ions.

The Freundlich model predicts the adsorption on a heterogeneous surface without saturation of adsorbent binding sites [21]:

$$\log q_e = \log k_f + (1/n) \log C_e$$

where K_F (mg g^{-1}) is a unit capacity coefficient and n is the Freundlich parameter related to the degree of system heterogeneity. The parameter n is usually greater than unity, and the larger it is, the more heterogeneous is the system [22]. The Langmuir model showed a good fit to the experimental data with higher R^2 in comparison to the Freundlich model.

The estimated Q_o values from Fig.8 were very close to the experimentally obtained maximum metal uptake, with Cu(II) and Zn(II) adsorption. For this adsorbent, a slightly higher Q_o value was estimated for Cu(II) than for Zn(II) (165.32and 124.5 mgg^{-1}, respectively), as observed experimentally. The Q_o of adsorbed Cu(II) was larger than that of Zn (II). The maximum adsorption capacity of Chitosan/silica composite adsorbent for the removal heavy metals is compared with other adsorbents reported in previous works, Table 3. It corresponded to the adsorption order observed experimentally: Cu(II)- grafted chitosan > Zn(II)- grafted chitosan.

Table 2. Langmuir and Freundlich adsorption constants associated to adsorption isotherms of Cu(II)and Zn(II) ions on Chitosan/silica composite.

Metal	Langmuir constants				Freundlich constants		
	Q_o (mg/g)	K_L	R_L	R^2	K_F	n	R^2
Cu(II)	161.44	0.17	0.63	0.99	13.44	0.88	0.92
Zn(II)	116.154	0.193	0.51	0.98	22.47	0.77	0.94

It can be concluded that the surfaces of modified chitosan had adsorption sites that were able to bind Cu(II) higher than that Zn(II) ions.

Table 3 comparison of the maximum adsorption capacity of heavy metals onto different adsorbents

Adsorbent	q_m (mg/g)	Ref.
chitosan/silica/ZnO nanocomposite	293.3	4
PVA/chitosan	151.0	8
PVA/TiO_2	187.6	10
EDTA-chitosan	63.0	33
Chitosan/silica composite	165.32	This study

3.8. Regeneration studies

Regeneration of the spent adsorbent is necessary to restore its original adsorption capacity and it enables valuable metals to be recovered from polluted water streams for reuse. In this study, Cu(II) and Zn(II) were desorbed from Chitosan/silica composite using 2M HNO3. From Table 4 we can suggest that the regeneration efficiency of adsorbents were almost complete for the metal. These results indicate the suitability of HNO_3 as the regenerator for the adsorbents. It seems that Chitosan/silica composite stabilized to resist acidic regenerate.

Table 4: Regeneration of Chitosan/silica composite for Cu(II) and Zn(II) by 2M HNO3

Type of adsorbent	No. of cycles	RE%	
		Cu(II)	Zn(II)
Chitosan/silica composite	1	99.00	98.60
	2	98.60	97.30
	3	98.50	97.00
	4	97.60	98.00
	5	98.50	97.60
	6	99.20	98.50

3.9. Application on a real polluted groundwater sample

Groundwater in El-Obor City is considered as one of the alternative sources of water supply for different purposes (such as domestic, livestock, and irrigation). The groundwater in the study area is extracted from the Miocene aquifer. The chemical analysis of the groundwater samples showed that the soluble iron and Zinc of some groundwater samples is exceeding the permissible limits for drinking (0.3 mg/l and 3 mg/l), respectively. To overcome this problem, two naturally occurring groundwater samples, which have higher iron and zinc concentrations, were chosen for the treatment process. The efficiency of the prepared Chitosan/silica composite was proved by performing the chemical analyses of such groundwater samples before and after treatment process. The results showed that the soluble iron and Zinc in the first

sample was 1.2 ppm and 3.8 ppm before treatment and decreased to 0.157 ppm ppm 0.64 ppm, respectively after treatment. The concentrations of iron and zinc in the second sample also decreased to 0.079 ppm and 0.69 after it was 0.938 ppm and 4.2 ppm, respectively before treatment process. It can be concluded that the surface of the prepared Chitosan/silica composite had adsorption sites that were able to bind iron and zinc ions.

4. Conclusions

Facile steps strategies for the surface modification of chitosan with silica nanoparticles were reported. The resulting Chitosan/silica composite removes heavy materials quickly and with high efficiently from polluted water. This paper suggested that this improved efficiency is due to the introduction of silica nanoparticles onto chitosan surface. Additionally, the reduced particle dimensions and high surface-to-volume ratio improved its efficiency as well. This study demonstrates that these chitosan-silica composite materials can be used as environmental friendly sorbents to efficiently remove heavy materials from water. A perspective for future studies involves adsorption kinetics followed pseudo-first-order and pseudo-second-order models for grafted chitosan, and kinetic data were better described by the pseudo-second-order model than by the pseudo-first-order model. Also the rate of the adsorption affected with pH and time. The adsorption studies in our system showed that the grafted chitosan had much better affinity for Cu(II) than for Zn(II) from the contaminated water. The Langmuir model showed a good fit to the experimental data with higher R^2 in comparison to the Freundlich model.

References

[1]. Sofia F. Soares, Margarida I. Rodrigues, TitoTrindade, Ana L. Daniel-da-Silva Chitosan-silica hybrid nanosorbents for oil removal from water *Colloids and Surfaces A: Physicochem. Eng.* doi:10.1016/j.colsurfa.2017.04.076.

[2]. Muzammil Anjum, R. Miandad, Muhammad Waqas, F. Gehany, M.A. Barakat Remediation of wastewater using various nano-materials doi.org/10.1016/j.arabjc.2016.10.004.

[3]. Angela Vionna Santoso, Alex Susanto, Wenny Irawaty, Lannie Hadisoewignyo, and Sandy Budi Hartono Chitosan modified mesoporous silica nanoparticles as a versatile drug carrier with pH dependent properties,AIP Conference Proceedings 2114, 020014 (2019)

[4] A. Salama, Preparation of CMC-g-P(SPMA) super adsorbent hydrogels: exploring

their capacity for MB removal from waste water, Int. J. Biol. Macromol. 106 (2018)

940–946.

[5] A. G, E. Skwarek, T.M. Budnyak, D. Ko, Metal ions removal using nano oxide Pyrolox

™material, Nanoscale Res. Lett. 12 (2017), 95.

[6] H. Hou, R. Zhou, P. Wu, L. Wu, Removal of Congo red dye from aqueous solution with hydroxyapatite/chitosan composite, Chem. Eng. J. 211–212 (2012) 336–342.

[7] A. Salama, Polysaccharides/silica hybrid materials: new perspectives for sustainable raw materials, J. Carbohydr. Chem. 35 (2016) 131–149.

[8]. Walcarius, A., & Mercier, L. (2010). Mesoporous organosilica adsorbents: nanoengineered materials for removal of organic and inorganic pollutants, Journal of Materials Chemistry, 20, 4478–4511.

[9]. Joo, J.B., Park, J., & Yi, J. (2009). Preparation of polyelectrolyte-functionalized mesoporous silicas for the selective adsorption of anionic dye in an aqueous solution, Journal of Hazardous Materials, 168, 102–107.

[10]. Niyaz Mohammad Mahmoodi , Zahra Mokhtari-Shourijeh, and Jafar AbdiPreparation of Mesoporous Polyvinyl Alcohol/ Chitosan/Silica Composite Nanofiber and Dye Removal from WastewaterEnvironmental Progress & Sustainable Energy (Vol.00, No.00) DOI (2018) 10.1002/ep.

[11]. Hazem Hassan , Ahmed Salama , Ahmed K. El-ziaty , Mohamed El-Sakhawy,New chitosan/silica/zinc oxide nanocomposite as adsorbent for dye removal, International Journal of Biological Macromolecules 131 (2019) 520–526.

[12] A. Salama, P. Hesemann, Synthesis of N-Guanidinium-chitosan/silica hybrid composites: efficient adsorbents for anionic pollutants, J. Polym. Environ. 26 (2018) 1986–1997,

[13]. F. Zhang, X. Chen, F. Wu, Y. Ji, High adsorption capability and selectivity of ZnO nanoparticles for dye removal, Colloids Surf. A Physicochem. Eng. Asp. 509 (2016) 474–483,

[14]. C. Flores, M. Lopez, N. Tabary, C. Neut, F. Chai, D. Betbeder, C. Herkt, F. Cazaux, V. Gaucher, B. Martel, and N. Blanchemain: Preparation and characterization of novel chitosan and b-cyclodextrin polymer sponges for wound dressing applications. Carbohydr. Polym. 173, 535 (2017).

[15].G.N. Kousalya, Muniyappan Rajiv Gandhi, S. Meenakshi, Sorption of chromium(VI) using modified forms of chitosan beads. International Journal of Biological Macromolecules 47 308–315 (2010).

[16] S. Azizian, Kinetic models of sorption: a theoretical analysis, J. Colloid Interface Sci. 276 (2004) 47–52.

[17] W. Rudzinski, W. Plazinski, Kinetics of solute adsorption at solid/solution interfaces: a theoretical development of the empirical pseudo-first and pseudosecond order kinetic rate equations, based on applying the statistical rate theory of interfacial transport, J. Phys. Chem. B 110 (2006) 16514–16525.

[18] W. Rudzinski, W. Plazinski, On the applicability of the pseudo-second order equation to represent the kinetics of adsorption at solid/solution interfaces: a theoretical analysis based on the statistical rate theory, Adsorption 15 (2009) 181–192.

[19] Ahmed M. Desouky, Mohamed E.A. Ali and Ehab ZaghloolAdsorption Of Heavy Metals From Groundwater Using Titanate NanoparticlesDoped With Cross-Linked Polyvinyl Alcohol. Bahr El-Baqar Drain Region, El-Husinia, East Delta-Egypt International Journal of Environment 09(2020) 148-158.

[20] W.H. Cheung, Y.S. Szeto, G. McKay, Intraparticle diffusion processes during acid dye adsorption onto chitosan, Bioresour. Technol. 98 (2007) 2897–2904.

[21]Eveliina Repoa,∗, Jolanta K. Warcholc, Tonni Agustiono Kurniawana,1, Mika E.T. SillanpaaaAdsorption of Co(II) and Ni(II) by EDTA- and/or DTPA-modified chitosan:Kinetic and equilibrium modeling Chemical Engineering Journal 161 (2010) 73–82

[22] D.D. Do, Adsorption Analysis: Equilibria and Kinetics, Imperial College Press, London, 1998.